https://doi.org/10.61092/iaea.gt8c-xz0h

INTERNATIONAL ATOMIC ENERGY AGENCY

NUCLEAR DATA SERVICES

DOCUMENTATION SERIES OF THE IAEA NUCLEAR DATA SECTION

IAEA-NDS-0239
April 2022

Fission Fragment Decay Calculation by the Hauser-Feshbach Statistical Decay Theory in TALYS 1.96

Kazuki Fujio
Tokyo Institute of Technology

Shin Okumura
and
Arjan Koning
IAEA Nuclear Data Section

Nuclear Data Section
International Atomic Energy Agency
P.O. Box 100
A-1400 Vienna
Austria

E-mail: nds.contact-point@iaea.org
Fax: (43-1) 26007
Telephone: (43-1) 2600 21725
Web: http://nds.iaea.org/

Disclaimer

Neither the author nor anybody else makes any warranty, expressed or implied, or assumes any legal liability or responsibility for the accuracy, completeness or usefulness of any information disclosed, or represents that its use would not infringe privately owned rights.

The IAEA-NDS would appreciate any comment on this report at: nds.contact-point@iaea.org.

Vienna, April 2022

Abstract

We calculate the deexcitation process of fission fragments based on the Hauser-Feshbach statistical decay theory which was implemented in the nuclear reaction code, TALYS. As the input of TALYS, fission fragment distribution parameters produced by three phenomenological and microscopic models, GEF, HF^{3}D, and SPY, are introduced. We review the calculated prompt neutron observables by comparing them with available experimental and evaluated nuclear data.

In this report, we describe (1) the method of the deterministic fission fragment distribution implemented in TALYS, (2) the fission fragment distribution parameters file, and show (3) the results on ^{239}Pu+n system at incident neutron energy at thermal to 5 MeV. In addition, we also examine (4) the practicality of TALYS-calculated independent fission product yields by calculating β-decay observables, cumulative fission product yield, decay heat, and delayed neutron yield, by the standalone Python code.

Table of contents

1 Introduction

In nuclear fission, a nucleus splits into two or smaller nuclei releasing about 200 MeV energy. It has been of interest for not only nuclear engineering applications but also the understanding of the rapid neutron-capture process (r-process) which is the nucleosynthesis proceeding in stellar environments. In nuclear fission, observables such as the fission product yields and the number of emitted neutrons are quite valuable information and have been measured especially for nuclear reactor operation and nuclear security.

Figure 1 shows the schematic view of the binary fission process. We divide the process into 3 main stages, (1) fission, (2) prompt decay, and (3) β decay.

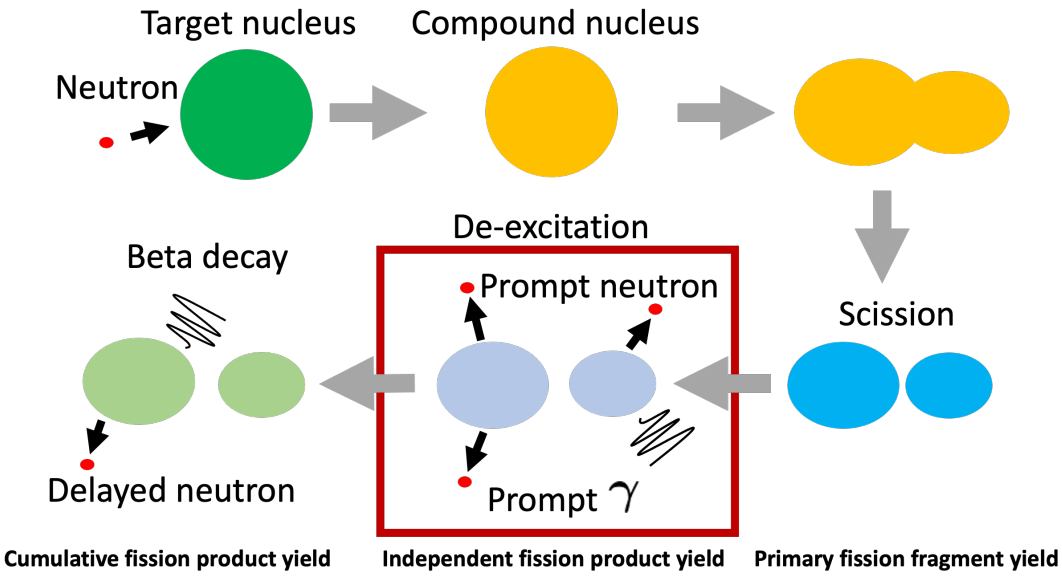

Figure 1: The process of fission reaction

(1) The fission process starts with forming a compound nucleus by capturing a neutron at a target nucleus and forming a compound nucleus (CN). The CN deforms and splits into two fragments (when the binary fission is taken into account) caused by the large-amplitude collective motion. There are many approaches to the theoretical description of nuclear fission such as fully microscopic models describing the fission process by assuming the nuclear interaction between the nucleons [1]. However, there have been limited experimental measurements performed to date, and the majority of the existing data is after the prompt and β decay which is not comparable to the yields calculated by fission theories. To compare the theoretical fission calculation with the experimental observables, prompt neutron and γ evaporation and β decay processes need to be taken into account, which are different processes from nuclear fission itself.

(2) Shortly after the scission, two split fragments accelerate due to their mutual Coulomb repulsion and are highly excited, triggering the emission of prompt neutrons and γ rays to reach the ground or metastable state. This process is generally simulated by the Hauser-Feshbach statistical decay theory [2] and/or phenomenological models to calculate prompt γ and neutron emission multiplicity and energy spectra as well as the independent fission product yield. The sequential emission of prompt neutrons and γ rays have been calculated with Monte Carlo approaches in CGMF [3] followed by many works of theoretical and phenomenological model developments such as FREYA[4], FIFRELIN[5], GEF[6], Point-by-Point[7], HF^{3}D[8, 9, 10],

and more works are underway. Until recently, most nuclear data evaluation works related to the prompt fission observables were limited to the average number (multiplicity) of prompt neutrons and γ rays, average energy distribution (spectrum), and fission product yields produced by combining experimental data and phenomenological models [11, 12], where more comprehensive models are desired.

(3) Most of fission products are unstable and therefore radioactive due to the excess of neutrons that lead to β^- decay. The fission products approach stable nuclides with rates depending on their β^--decay half-lives and the fission product yields cumulated at a certain time is called cumulative fission products. While β decaying, the β and γ heats released as a result of β^- decay and some delayed neutrons emitted from the neutron-rich fission products are also important because they are precisely measurable fission observables.

The Nuclear Data Section in the IAEA initiated the Coordination Research Project on "Updating fission product yield data for applications"[13]. The project reviews the current possible theoretical and phenomenological fission and decay models that have been advanced in the past decades. In line with the CRP activities, the nuclear reaction code, TALYS [14], we added a new feature to calculate independent fission product yield and prompt fission observables from fission fragments based on the Hauser-Feshbach statistical decay theory [2]. In the current version of TALYS (later than version 1.96), three different fission fragment distribution models are prepared. In this report, we explain the outline of each fission fragment model, and how they work in TALYS, and we report calculated results compared with experimental and evaluated data. In addition to that, we also report the β-decay observables calculated by a standalone Python β-decay code using calculated independent fission product yields by TALYS.

2 The Hauser-Feshbach statistical decay theory for the fission fragment deexcitation

2.1 Deexcitation of fission fragment

Highly excited fission fragment deexcites by emitting neutrons and γrays. The probabilities of neutron and γ-ray emissions from fission fragment as a compound state are calculated with neutron and γ-ray transmission coefficients, where the particle and γ competition is always included at each stage of the compound nucleus decay, as shown in Fig. 2. The model can predict prompt particle emission spectra, probabilities, and multiplicities, then $Y_I(Z, A)$, simultaneously by integrating over the distribution of initial configurations.

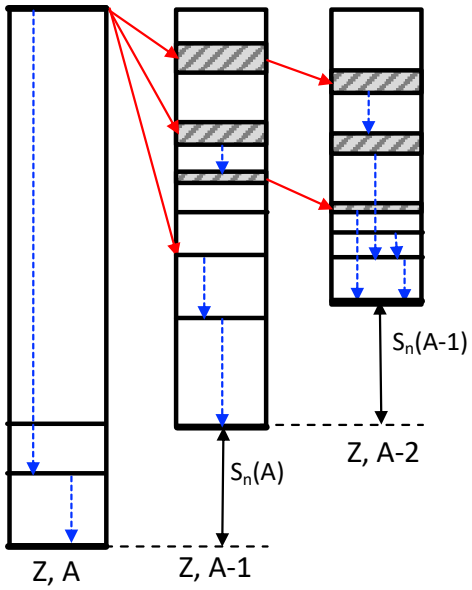

Figure 2: Schematic view of the multiple neutron and γ-ray emission process from a compound nuclide (CN), (Z,A). The solid arrows represents the neutron emission, and the dotted arrows represents the γ-ray emission.

To perform such Hauser-Feshbach statistical decay calculation, an initial configuration of each fission fragment, namely $Y_{\rm ff}(Z, A, E_x, J, \Pi)$ of fragment yield $Y_{\rm ff}$, charge Z, mass A, excitation energy E_x, spin J, and parity Π distributions are required. These distributions are often obtained by some theoretical and/or phenomenological models for the dynamical fission process. Instead of performing the integration, several Monte Carlo (MC) tools have been developed to calculate the fission deexcitation process and to reproduce these observables. Although the MC technique gives correlations in the prompt particle emissions, its lengthy computation makes it difficult to reproduce an extremely small probability of fission fragment production and it never samples such a case in a reasonable computational time.

Recently, the Hauser-Feshbach statistical decay theory [2] applied for the fragment deexcitation process has been implemented in the HF^{3}D model [8] using a phenomenological fission fragment distributions fitted by the experimental $\rm Y_{ff}(A)$ and TKE data, which is described in the Section 3.5. The methodology used in this report implemented in TALYS is to apply the deterministic technique that produces the fission fragment distribution deterministic manner in the same methodology as HF^{3}D model, but read the distribution from the file that stores the fission fragment distribution parameters.

2.2 Prompt decay physical quantities

The results of statistical decay calculations may be post-processed to construct some fission quantities, which are then compared with available experimental data. Typical quantities that are often given in the literature are summarized in Table 1. In this report, we limit to examining prompt neutron observables.

Table 1: Representative fission quantities comparable to experimental data.

Type	Description
$Y_i(A)$	Independent fission yield as a function of mass number
$Y_i(Z, A, M)$	Independent fission yield of all isotopes including meta-stable state
$\overline{\nu}$	Average number of neutrons per fission
$\overline{\gamma}$	Average number of γ-rays per fission
$\overline{\nu}(A)$	Average neutron multiplicity as a function of fission product mass
$\overline{\gamma}(A)$	Average γ-ray multiplicity as a function of fission product mass
$\langle E_n \rangle$	Average prompt neutron energy
$\langle E_\gamma \rangle$	Average prompt γ-ray energy
$\langle E_n \rangle(A)$	Average neutron energy as a function of product mass
$\langle E_\gamma \rangle(A)$	Average γ-ray energy as a function of product mass
P(ν)	Neutron multiplicity distribution
$\chi(\nu)$	Prompt fission neutron energy spectrum (PFNS)
$\phi(\gamma)$	γ-ray energy spectrum

3 Fission fragment distribution models in TALYS

3.1 General description

The deexcitation of the fission fragments by the Hauser-Feshbach statistical decay theory is implemented in TALYS (later than version 1.96). As explained in Section 2.1, the methodology used here is to apply the deterministic technique for primary fission fragment decay calculation similar to the HF^{3}D model [8]. In order to calculate the deexcitation of the fission fragment, input of the initial conditions, namely $Y_{\rm ff}(Z, A, E_x, J, \Pi)$, are necessary.

Recently, Nordström et al. [15] produced a substantial fission fragment distribution dataset for more than 700 fissionable nuclides for the 0–25 MeV incident neutron energy range for fissionable isotopes ranging from Os to Mc by the GEF code [6]. Including the GEF produced dataset mentioned above, TALYS incorporates three fission fragment distribution parameters dataset produced by GEF [6, 15], HF^{3}D [8, 9, 10], and Scission Point Yield (SPY) [16] models, so far. The HF^{3}D model is available for ^{235}U, ^{238}U, and ^{239}Pu. The SPY model is available for Am and Pu isotopes. The covered nuclides are shown in Fig. 3. The user can specify the fission fragment model in TALYS input with `ffmodel` keyword (See TALYS manual and Section 3.3 for details).

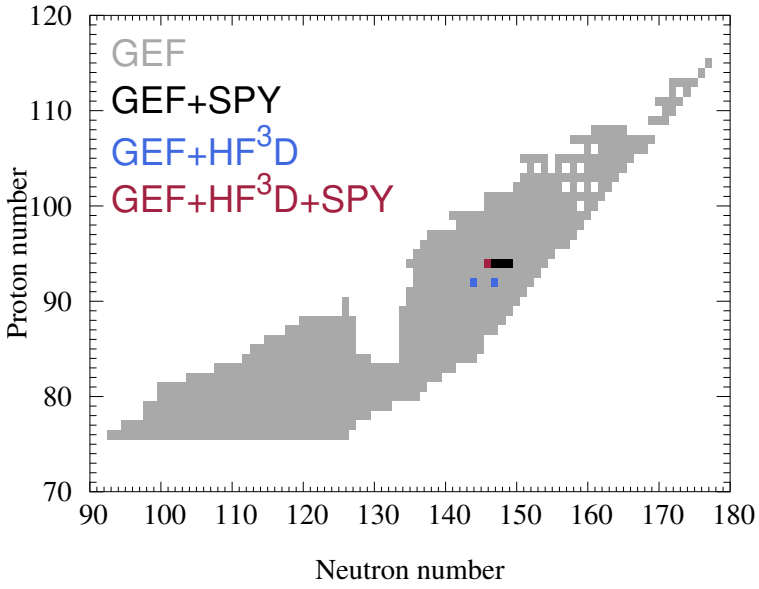

Figure 3: Valid range of each model.

The available models, compound nuclides, and energy ranges are expected to be extended and be updated from time to time.

Brief descriptions for the three models will be given in Section 3.4,3.5 and 3.6.

3.2 Fission fragment distribution parameter file

The fission fragment distribution parameters generated by above models are stored in a tabulated format file in

`/talys/structure/fission/ff/ffmodel/`,

where `ffmodel` can be "gef", "hf3d", or "spy" for three models mentioned above. The file name must consist of 3 fields, `CN`, `energy`, and type of `ffmodel` such as

`/talys/structure/fission/ff/ffmodel/Elaaa/Elaaa_energyMEV_ffmodel.ff`,

where `El` and `aaa` stand for the element with capitalize the first letter and mass number in 3 digit for CN, `energy` stands for the sum of the neutron separation energy (S_N) of CN and the incident neutron energy ($E_{\rm in}$) in case of the neutron induced reaction.

The example of the file format, which is inspired by the format used in the HF^{3}D model [8], for ^{235}U+$n_{\rm thermal}$ reaction from the GEF model is shown below as an example.

```
# Z        =   92
# A        =  236
# Ex (MeV) = 6.55e+00
# Ntotal   =  195
# Zl  Al  Zh  Ah  Yield       TKE[MeV]    TXE[MeV]    El[MeV]     Wl[MeV]     Eh[MeV]     Wh[MeV]
  30  74  62 162  3.0000e-06  1.4373e+02  2.5550e+01  9.7733e+00  1.7875e+00  1.5777e+01  5.7377e+00
  30  75  62 161  1.1000e-05  1.4544e+02  2.2786e+01  5.7400e+00  3.1184e+00  1.7046e+01  6.9337e+00
  31  75  61 161  2.0000e-06  1.4076e+02  2.6930e+01  5.7300e+00  5.5013e+00  2.1200e+01  2.4042e+00
  30  76  62 160  5.0000e-05  1.4532e+02  2.6206e+01  6.1234e+00  2.4469e+00  2.0082e+01  6.5358e+00
                        (omission of a middle part)
  46 117  46 119  9.0000e-05  1.6262e+02  3.4208e+01  1.7155e+01  8.5389e+00  1.7053e+01  7.6726e+00
  47 117  45 119  7.0000e-06  1.6130e+02  3.2700e+01  1.9750e+01  7.0597e+00  1.2950e+01  4.2823e+00
  45 118  47 118  7.0000e-06  1.6167e+02  3.1759e+01  1.4299e+01  1.0776e+01  1.7460e+01  8.7686e+00
  46 118  46 118  9.0000e-05  1.6435e+02  3.5416e+01  1.7522e+01  6.7362e+00  1.7893e+01  7.0032e+00
  47 118  45 118  1.1000e-05  1.6072e+02  3.2713e+01  1.6269e+01  5.4600e+00  1.6444e+01  7.6689e+00
```

The first 5 lines represent the information of the reaction; the charge Z, the mass A of a CN in (13x,i4) format, excitation energy E_x which is a sum of neutron separation energy S_N and incident neutron energy $E_{\rm in}$ of the compound nucleus in (13x,e8.2) format, and the number of fragment pairs $Ntotal$ in (13x,i4) format. In the numerical part, $Z_{l,h}$, $A_{l,h}$, and $Yield$ are the charge, mass, and yield of the complemental fission fragments that are supposed to be symmetric with respect to $A_{\rm CN}/2$. Therefore,

$$Y_{\rm ff}(Z_l, A_l) = Y_{\rm ff}(Z_{\rm CN} - Z_l, A_{\rm CN} - A_l) = Y_{\rm ff}(Z_h, A_h)\ , \tag{1}$$

where CN, l, and h denote the compound nucleus, light, and heavy fragment. TKE and TXE are the mean value of total kinetic energy and total excitation energy, and $E_{l,h}$ and $W_{l,h}$ are the Gaussian mean and width of the partitioned TXE into two fragments. Therefore,

$$E_l + E_h = TXE\ . \tag{2}$$

TALYS reads these parameters for each fission fragment from the file and reconstructs the excitation energy distribution $G_{l,h}(E_x)$ assumed to be a Gaussian form expressed as

$$G_{l,h}(E_x) = \frac{1}{\sqrt{2\pi}W_{l,h}} \exp\left\{-\frac{(E_x - E_{l,h})^2}{2W_{l,h}^2}\right\}. \tag{3}$$

The spin distribution $R(J,\Pi)$, which is the probability of having the state of J and Π, is assumed to be proportional to the available spin states in the level density formula

$$R(J,\Pi) = \frac{J+1/2}{2f^2\sigma_{l,h}^2(U)} \exp\left\{-\frac{(J+1/2)^2}{2f^2\sigma_{l,h}^2(U)}\right\}\ , \tag{4}$$

where $\sigma_{l,h}^2(U)$ is the spin cutoff parameter that can be altered by a keyword `Rspincut` which is set to 1 by default, f^2 is the global adjustable constant for the spin cutoff parameter for fission fragments that can be altered by a keyword `Rspincutff` set to 9 by default following Ref. [8],

and U is the excitation energy corrected by the pairing energy. After creating an initial population $P(E_x, J, \Pi) = R(J, \Pi)G_{l,h}(E_x)$ for the individual fission fragment, the Hauser-Feshbach statistical decay calculation is performed for each fission fragment. An optical potential for neutron, γ-ray strength functions, and nuclear level densities are also essential ingredients for such decay calculations. For them, TALYS reads information from RIPL-3 [17].

In case the exact $E_{\rm in}$ that the user specified in the input is not available, TALYS interpolates the distribution between the nearest energy files. Some models are available for $E_{\rm in} > 5$ MeV, but we haven't examined above 5 MeV at the time of compilation of this report, since the fission fragment decay including the multi-chance fission has not yet been implemented.

3.3 TALYS input

The fission fragment model can be specified in the TALYS input, for example, `ffmodel 1` for GEF, `ffmodel 2` for HF^{3}D, and `ffmodel 3` for SPY model. The fission fragment deexcitation by the Hauser-Fesbach statistical decay needs to be specified by setting `fymodel 4`.

The following example shows typical input keywords to calculate ^{239}Pu(n$_{\rm th}$,f) observables that takes fission products with yield more than 1.0E-09 into account and outputs spectra and mass distribution in separate files.

```
projectile   n
element      Pu
mass         239
energy       2.53E-8
ejectiles    g n
filespectrum g n
massdis      y
ffmodel      1
fymodel      4
Rfiseps      1.0e-9
outspectra   y
bins         60
channels     y
maxchannel   8
```

The input keyword that can affect on the calculated fission observables significantry are `bins`, `ldmodel`, and `Rfiseps`. We also report the sensitivities over these two parameters in Section 4.3.

3.4 GEF model

The GEF code [6] is the fission modelling code that attempts to provide a general description of fission observables based on benchmarking the model with empirical datasets. The GEF code calculates the fission observables based on the Monte Carlo sampling, which preserves the event-by-event correlation between fission observables, such as fragment yields and kinetic energies and the kinematics of fragments and emitted particles. A macroscopic approach is utilized by deriving global fit parameters to a large set of experimental data such as fission mass and charge yields, prompt fission neutrons, and gamma rays. The code estimates fission barrier heights from the topographic theorem and derives fission fragment yields by utilizing the Brosa model [18] with Gaussian fitting. It estimates the sharing of available energy (Q value) between Total Kinetic Energy (TKE) and Total Excitation Energy (TXE). It further employs statistical mechanics and the law of entropy to share the excitation energy between the fragments. The TXE partitioning is determined according to a probability distribution that is given by the product of the level densities of the individual fragments [19].

Nordström et al. [15] used GEF as a fission event generator and performed 1,000,000 random samplings. Then the Python script was used to calculate the average TKE and TXE of the fission fragment pair, and to produce mean and standard deviations, $E_{l,h}$ and $W_{l,h}$, of light and heavy fragments from the list mode output file.

Figure 4 shows the fission fragment mass distribution for ^{240}Pu(n,f) constracted from the Nordström's data.

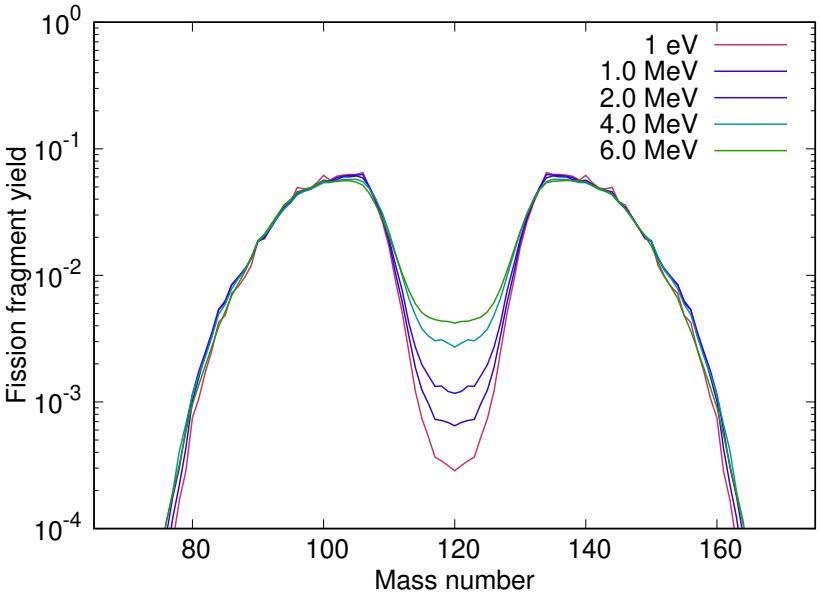

Figure 4: The energy dependence of fission fragment yield with logarithmic scale for ^{240}Pu(n,f) with incident neutron energies from 1 eV to 5 MeV generated by the GEF code [15].

3.5 HF^{3}D model

The Hauser-Feshbach fission fragment decay model (HF^{3}D) [8, 9, 10] has been developed based on the full deterministic technique to calculate fission observables. In the HF^{3}D model, the primary fission fragment yield $Y(A)$ and TKE are determined by fitting experimental data with simple analytical functions. In order to generate charge distribution $Y(A, Z)$, Z$_P$ model [20] is employed, and the excitation energy divide is made by the anithothermal model [21] to reproduce $\overline{\nu}(A)$. For the TALYS fission fragment distribution parameter dataset, 3 compound nuclides, ^{235}U, ^{238}U, and ^{239}Pu, for which some fittable experimental data exist, are provided. The details of the HF^{3}D model are explained below.

The fission fragment mass distribution $Y(A)$ is made of the sum of multi (5 or 7) Gaussian functions.

$$Y(A) = \sum_{i=1}^{5} \frac{Y_i}{\sqrt{2\pi}\sigma_i} \exp\left\{ -\frac{(A - A_m + \Delta_i)^2}{2\sigma_i^2} \right\}, \tag{5}$$

where σ_i and Δ_i are the Gaussian parameters, A_m $(= A_c/2)$ is the symmetry point of the mass distribution, and Y_i is the component of yield. Y_i is divided into the principal peak curves $Y_{1,5}$, the inner peak curves $Y_{2,4}$, and the central peak curve Y_3.

Principal curves

$Y_{1,5}$ are the main component of the mass distribution for high and low energy fission, and

The shape of curves depends on the charge of the fissile nuclide Z_F and the precursor excitation energy (the projectile incident energy E_{inc} plus the separation energy S_N)

Inner peak curves

$Y_{2,4}$ especially affects the shape of mass distribution for $A_h = 130$ and $A_l = A_c - 130$. The large kinetic energies and the small amount of the prompt neutron emission derives in $Y_{2,4}$.

Central peak curve

The intensity of Y_3 increases with getting the precursor excitation energy bigger.

The Gaussian parameters are determined with the least square method.

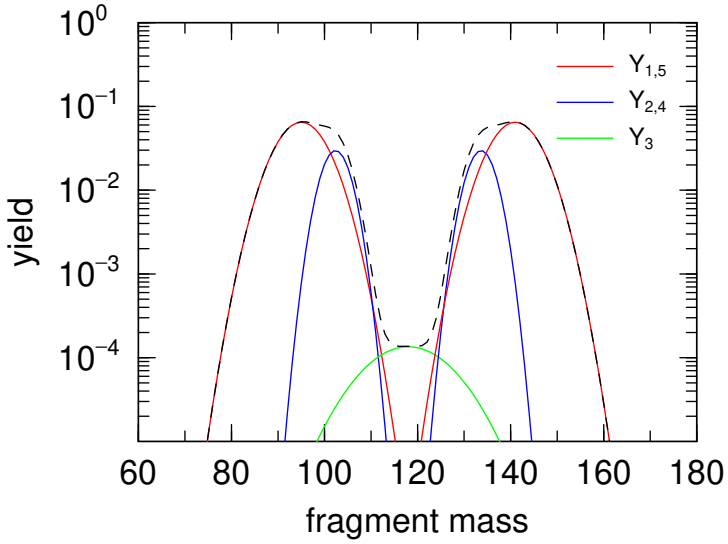

Figure 5: Fission fragment yield defined in the HF^{3}D model. Solid lines represent each Gaussian component and the dashed line is the sum of these Gaussians.

Every $Y(A)$ has the charge distribution and Wahl's Z_P model [22] is employed to get yield $Y(A, Z)$ in HF^{3}D model. The Z_P model treats a dispersion of fractional independent yields of primary fission products with Z for each A. In this calculation, this yield is regarded as the fragment yield. Gaussian dispersion, modified for even-odd proton and neutron effects, is assumed. Parameters for the model are determined by the method of least squares from fractional independent and fractional cumulative yield values derived from experimental data. The equations are shown with the error function of x, $erf(x)$:

$$\begin{aligned} Y(A,Z) &= 0.5F(A)N(A)\left\{erf(V) - erf(W)\right\}, \\ V &= \frac{Z(A) - Z_p(A) + 0.5}{\sigma_Z(A)\sqrt{2}}, \\ W &= \frac{Z(A) - Z_p(A) - 0.5}{\sigma_Z(A)\sqrt{2}}, \\ Z_p(A_{l,h}) &= Z_{\mathrm{UCD}}(A_{l,h}) \pm \Delta Z(A_{l,h}), \\ &= A_{l,h} \times Z_c/A_c \pm \Delta Z(A_{l,h}). \end{aligned} \tag{6}$$

where $N(A)$ is the normalization factor, and $F(A)$ is the even-odd factor. As shown below, this factor is distinguished by even or odd for neutron and proton numbers. Parameters

for Z	for N	$F(A)$
even	even	$F_Z(A) \times F_N(A)$
even	odd	$F_Z(A)/F_N(A)$
odd	even	$F_N(A)/F_Z(A)$
odd	odd	$1/\{F_Z(A) \times F_N(A)\}$

Table 2: The even-odd factors for the fission fragment yield

$\sigma_Z, \Delta Z, F_Z, F_N$ and their slopes with respect to A are determined in contiguous regions of A for each fission reaction by the method of least squares. $Z_p(A_{l,h})$ is the most probable charge in the fission fragment. In the UCD (Unchanged Charge Distribution) assumption, $Z_p(A_{l,h})$ is the same charge proportion as its fissile nuclide. However, the actual Z_P seems to be different from $Z_{\rm UCD}$, the charge from UCD approximation, and the difference between actual one and UCD one is called the charge polarization ΔZ.

The total kinetic energy TKE is given by a Gaussian function:

$$\begin{aligned} \mathrm{TKE}(A_h) &= (p_1 - p_2 A_h)\left\{1 - p_3 \exp\left(-\frac{(A_h - A_m)^2}{p_4}\right)\right\} + \varepsilon_{\rm TKE} \\ &\propto \exp\left(-\frac{(A_h - A_m)^2}{2W_{\rm TKE}^2}\right) \end{aligned} \tag{7}$$

where p_1, p_2, p_3, and p_4 are fitting parameters and $\varepsilon_{\rm TKE}$ is a small correction. Both parameters are fitted to agree with evaluated $\overline{\rm TKE}$. Moreover, TKE is also represented with a width parameter $W_{\rm TKE}$ which is empirically known to be about 8-10 MeV. The total excitation energy TXE which is shared with the light and heavy fragments is shown with this TKE,

$$\begin{aligned} \mathrm{TXE}(A_l, Z_l; A_h, Z_l) &= Q_f(A_l, Z_l; A_h, Z_l) - \mathrm{TKE}(A_l, Z_l; A_h, Z_l) \\ &= [M_n(A_c, Z_c) - M_n(A_l, Z_l) - M_n(A_h, Z_h)]\, c^2 \\ &\quad + E_{inc} + S_n - \mathrm{TKE}(A_l, Z_l; A_h, Z_l), \end{aligned} \tag{8}$$

where Q_f is the Q value of the fission reaction, and M_n represents the nuclear mass. The TXE is distributed using the R_T parameter which is defined as the ratio of effective temperatures in the fission fragments,

$$R_T = \frac{T_l}{T_h} = \sqrt{\frac{E_l}{E_h}\frac{a_h(E_h)}{a_l(E_l)}}, \tag{9}$$

where $a_{l,h}(E_{l,h})$ are the level density parameters related to shell correction at $E_{l,h}$. Therefore, the energies are:

$$E_h = \mathrm{TXE}\frac{a_h}{R_T^2 a_l + a_h}, \qquad E_l = \mathrm{TXE}\frac{R_T^2 a_l}{R_T^2 a_l + a_h}. \tag{10}$$

The TXE distribution G is also represented by a Gaussian but the width is different from the width $W_{\rm TXE}$ which propagates from $W_{\rm TKE}$ due to the R_T;

$$G(E_x) = \frac{1}{\sqrt{2\pi} W_{l,h}} \exp\left\{-\frac{(E_x - E_{l,h})^2}{2W_{l,h}^2}\right\}. \tag{11}$$

In (11), $W_{l,h}$ is

$$W_{l,h} = \frac{W_{\mathrm{TXE}}}{\sqrt{E_l^2 + E_h^2}} E_{l,h} \qquad (W_{\mathrm{TXE}} = W_{\mathrm{TKE}}). \tag{12}$$

Figure 6 shows the fission fragment mass distribution for ^{240}Pu(n,f) used in Ref. [9] and are imported to TALYS fission fragment distribution dataset.

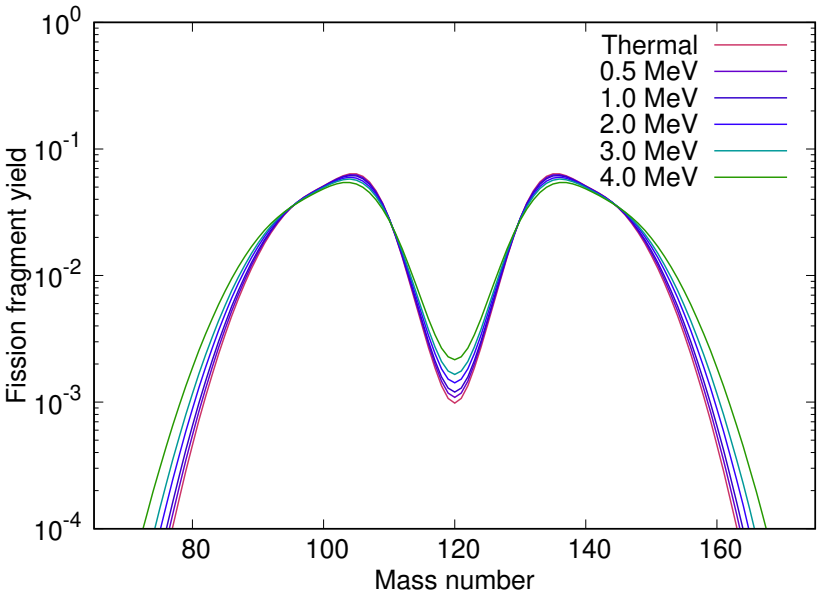

Figure 6: The energy dependence of fission fragment yield with logarithmic scale for ^{240}Pu(n,f) with incident neutron energies from thermal to 5 MeV provided from the HF^{3}D model [9].

3.6 SPY model

The SPY model [16] is a static and statistical scission-point model that assumes a statistical equilibrium at scission. This model is fully based on microscopic inputs, computed within the constraint Hartree-Fock-Bogoliubov (HFB) mean-field model using the Skyrme BSk27 [23] nucleon-nucleon effective interaction. This interaction can predict all the 2353 experimental masses with a root-mean-square deviation of 0.5 MeV and also describe infinite homogeneous nuclear matter properties. The main advantage of using the HFB model is it can describe nuclear structure properties for a wide range of nuclei without phenomenological parameters apart from those of the effective interaction.

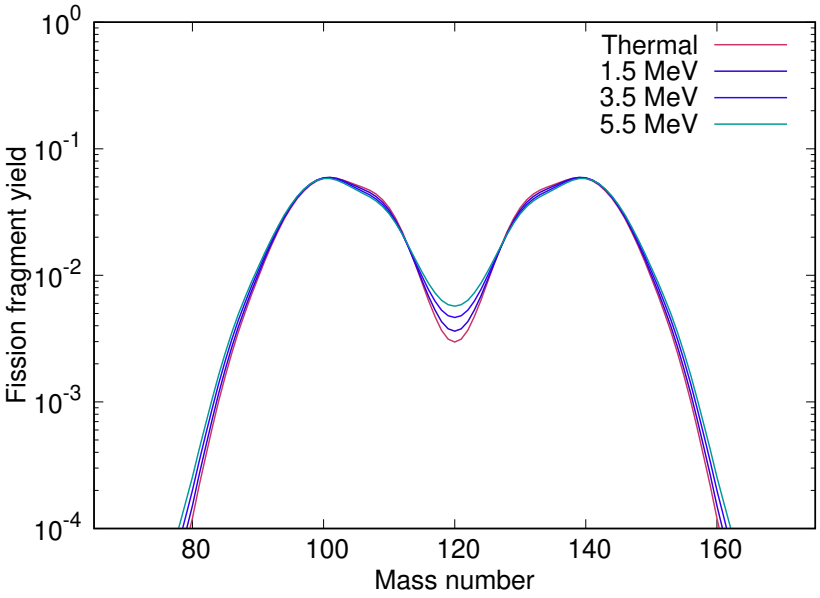

Figure 7: The energy dependence of fission fragment yield with logarithmic scale for ^{240}Pu(n,f) with incident neutron energies from thermal to 5 MeV generated by the SPY model [24].

In the SPY model, the scission configuration is defined by the proton density at the scission neck of the fissioning nucleus. The fission fragment yields are obtained by counting the number of available states at scission for all possible fragmentations. In regard, TKE is defined as the mean value of Coulomb repulsion plus nuclear attraction energy between fragments. TXE is the sum of the deformation energy and the intrinsic energy of the fission fragment pair. As TALYS input, the SPY model provides pre-neutron fission yields of 4 compound nuclei with excitation energies ranging from 0 to 20 MeV with a step of 2 MeV.

Figure 7 shows the fission fragment mass distribution for ^{240}Pu(n,f) that are imported into TALYS fission fragment distribution dataset [24].

3.7 User's model

In the latest TALYS, users can also introduce their own fission fragment distributions by preparing the same format and by setting `ffmodel 0` in the input as shown below as an example.

```
projectile   n
element      U
mass         235
energy       2.53E-8
ejectiles    g n
massdis      y
ffmodel      0
fymodel      4
Rfiseps      1.e-9
outspectra   y
bins         60
channels     y
maxchannel   8
```

The guidance is explained in the below Section 3.7.1 and 3.7.2.

3.7.1 Filename convention

For example, user can produce and store the fission fragment parameters in

`/talys/structure/fission/ff/local/.`

For the case of thermal neutron induced fission of Am242, file name should be

`/talys/structure/fission/ff/local/Am243/Am243_8.36e+00MeV_local.ff`.

Note that Am243 is the CN of this reaction. The excitation energy, 8.36e+00 MeV, is the sum of S_N of CN and $E_{\rm in}$, namely, $S_n + E_{in} = 8.36\,\mathrm{MeV} + 2.58 \times 10^{-8}\,\mathrm{MeV}$. `local` is the fixed keyword for the user's model and should be in lowercase. Underscores, "_", are necessary for the separation of fields. The extension must be "ff".

The S_N of Am243 can be easily check either by TALYS calculation using following keywords as input, from Live Chart of Nuclide [1], or from LANL S_N calculator [2].

```
Projectile g
Element    Am
Mass       243
Energy     0.1
Spherical  y
Outbasic   y
```

3.7.2 File format

The first 5 lines are the information of this input: the charge Z, the mass A of the CN, excitation energy E_x which is a sum of incident neutron energy and neutron separation energy of compound nucleus, and the number of fragment pairs $Ntotal$.

```
# Z        =   92
# A        =  236
# Ex (MeV) = 6.55e+00
# Ntotal   =  195
# Zl  Al  Zh  Ah  Yield       TKE[MeV]    TXE[MeV]    El[MeV]     Wl[MeV]     Eh[MeV]     Wh[MeV]
  30  74  62 162  3.0000e-06  1.4373e+02  2.5550e+01  9.7733e+00  1.7875e+00  1.5777e+01  5.7377e+00
  30  75  62 161  1.1000e-05  1.4544e+02  2.2786e+01  5.7400e+00  3.1184e+00  1.7046e+01  6.9337e+00
  31  75  61 161  2.0000e-06  1.4076e+02  2.6930e+01  5.7300e+00  5.5013e+00  2.1200e+01  2.4042e+00
  30  76  62 160  5.0000e-05  1.4532e+02  2.6206e+01  6.1234e+00  2.4469e+00  2.0082e+01  6.5358e+00
  31  76  61 160  3.0000e-06  1.4263e+02  2.5660e+01  6.4367e+00  5.2480e+00  1.9223e+01  6.4374e+00
  32  76  60 160  2.0000e-06  1.4519e+02  2.4145e+01  7.6750e+00  1.6617e+00  1.6470e+01  3.2103e+00
  30  77  62 159  4.0000e-05  1.4511e+02  2.4878e+01  5.8477e+00  3.0190e+00  1.9031e+01  7.3666e+00
  31  77  61 159  4.6000e-05  1.4866e+02  2.2875e+01  5.2296e+00  2.7442e+00  1.7646e+01  6.6627e+00
  29  78  63 158  3.0000e-06  1.3886e+02  2.1887e+01  3.8267e+00  1.5105e+00  1.8060e+01  1.2674e+01
```

There are some pointers on the preparation of user's model files and to read files from TALYS correctly.

Format

In the fourth line of the format, the number of fragment pairs is required to run calculations.
Z, A: format must be (13x,i4).
E_x: format must be (13x,e8.2).
$Ntotal$: format must be (13x,i4).
Column header should be at line 5.

File name

Each fission fragment file includes the sum of the projectile incident energy and the neutron separation energy in the title. TALYS calculates neutron separation energy and refers to the title when TALYS reads fission fragment files. Therefore, we need to pay attention to the title when fission fragment files are prepared.

[1] https://nds.iaea.org/livechart
[2] https://t2.lanl.gov/nis/data/astro/molnix96/sepn.html

.E file

Each nuclide directory must have a .E (*i.e.* Energy) file. In this file, available E_x, which is the sum of the neutron separation energy of CN and projectile incident energy should be listed. This file will be used when TALYS reads fission fragment files and interpolates between energies. For the case of the Am243 as CN, the file name must be `/talys/structure/fission/ff/local/Am243/Am243_local.E`.

```
6.53e+00
7.03e+00
7.53e+00
8.53e+00
1.05e+01
1.25e+01
1.65e+01
2.05e+01
2.65e+01
```

4 Calculated results

The calculated results of (1) the independent fission product yield $Y_{\mathrm{I}}(A)$, (2) the probabilities of prompt fission neutron multiplicity P_ν, (3) the number of prompt fission neutron as a function of fragment mass $\overline{\nu}(A)$, and (4) the prompt fission neutron spectra (PFNS) at the incident energy $E_{inc} = 0.0253$ eV (thermal) are compared with experimental and evaluated data.

Figure 8 shows $Y_{\mathrm{ff}}(A)$ at thermal neutron energy and the results are shown in Section 4.1.

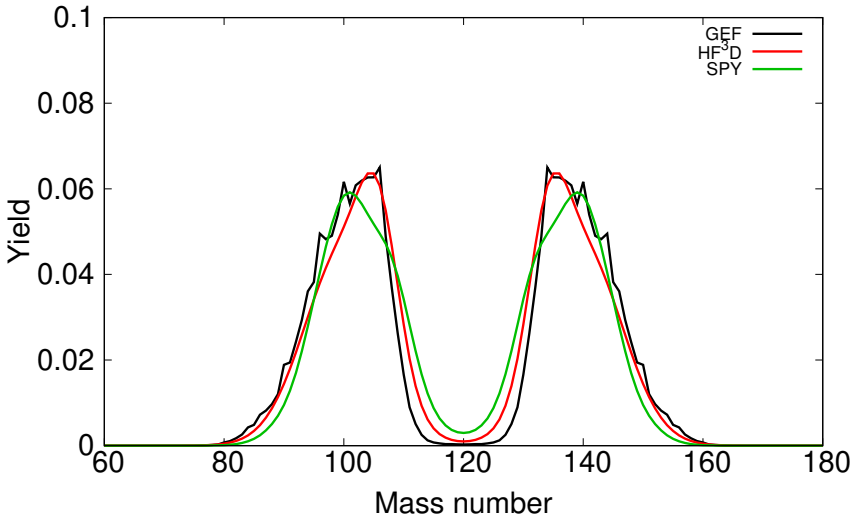

Figure 8: The fission fragment yields $Y_{\mathrm{ff}}(A)$ of three models are shown for comparison.

4.1 Thermal neutron induced fission

Figure 9 shows the calculated $Y_{\mathrm{I}}(A)$ together with experimental and evaluated data. The qualitative shape of the fragment yield is good in all models. The peak positions of $Y_{\mathrm{I}}(A)$, especially for the GEF and HF^{3}D model, are in good agreement with experimental and evaluated data. The peak positions of GEF and HF^{3}D are around $A = 135$ whereas that of the SPY is around $A = 140$. This difference brings disagreement also with other fission observables.

The calculated $\overline{\nu}$ are summarized in Table 3 and $\overline{\nu}(A)$ are shown in Fig. 10. Rhe SPY model shows large $\overline{\nu}(A)$ around $A = 130$, which may lead the large $\overline{\nu}$ in total. Figire 11 shows the calculated P_ν and the SPY model is approximately 1 larger neutron emission probabilities than other models.

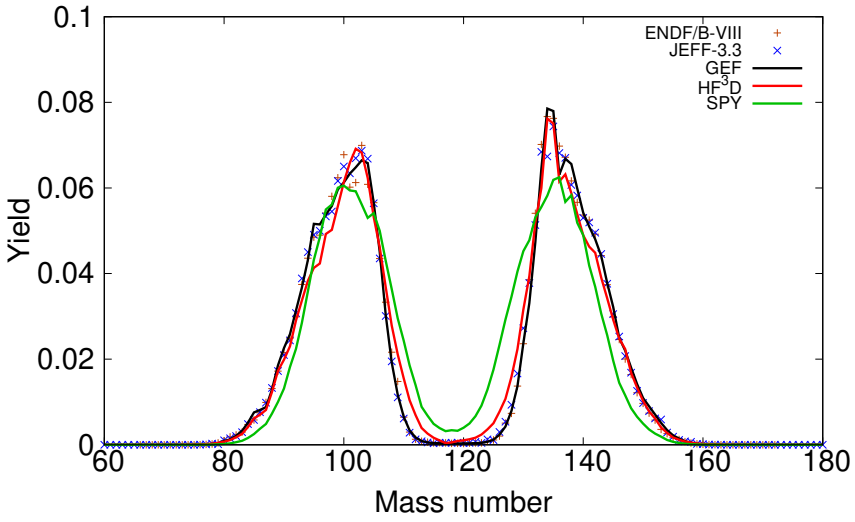

Figure 9: The calculated independent fission product yields $Y_{rmI}(A)$ shown together with the evaluated and experimental data for ^{240}Pu(n_{th},f).

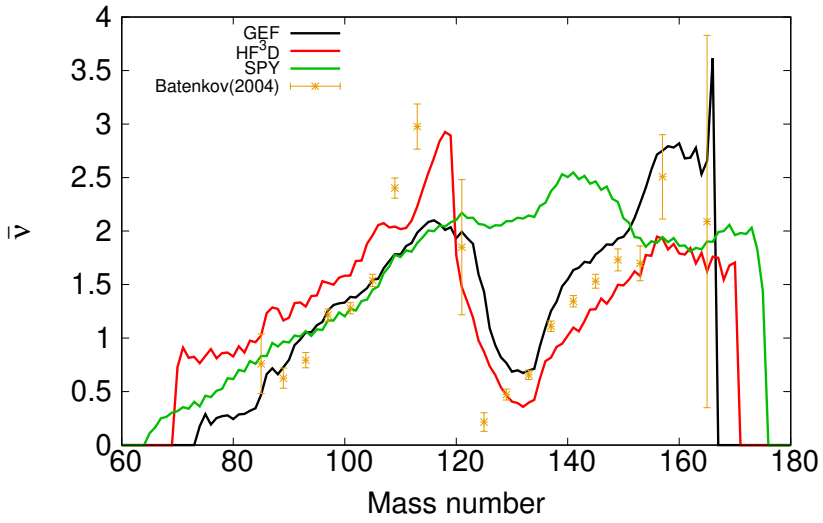

Figure 10: Rhe number of prompt fission neutron $\bar{\nu}(A)$ compared with experimental data.

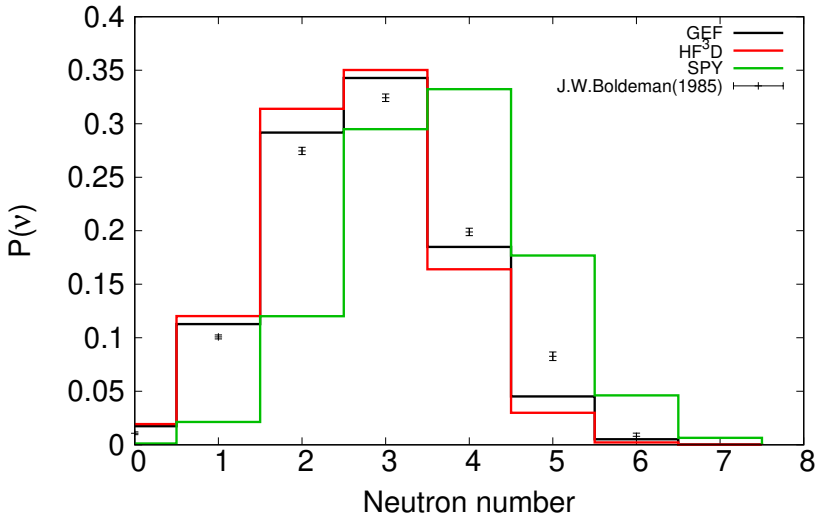

Figure 11: The prompt fission neutron multiplicity P_ν.

Table 3: The calculated average number of fission neutrons $\overline{\nu}$ at thermal energy compared with the evaluated value in ENDF/B-VIII and JENDL-4.0.

GEF	HF^3D	SPY	ENDF/B-VIII	JENDL-4.0
2.72	2.62	3.69	2.870488	2.87234

Figure 12 and 13 represent PFNS with a logarithmic scale and ratios to the Maxwellian at the temperature of 1.32 MeV. Although the calculation results seem to agree with the evaluated data in the logarithmic scale, the bump appears at around 2 MeV in all TALYS calculation results as ratios to Maxwellian at the temperature of 1.32 MeV.

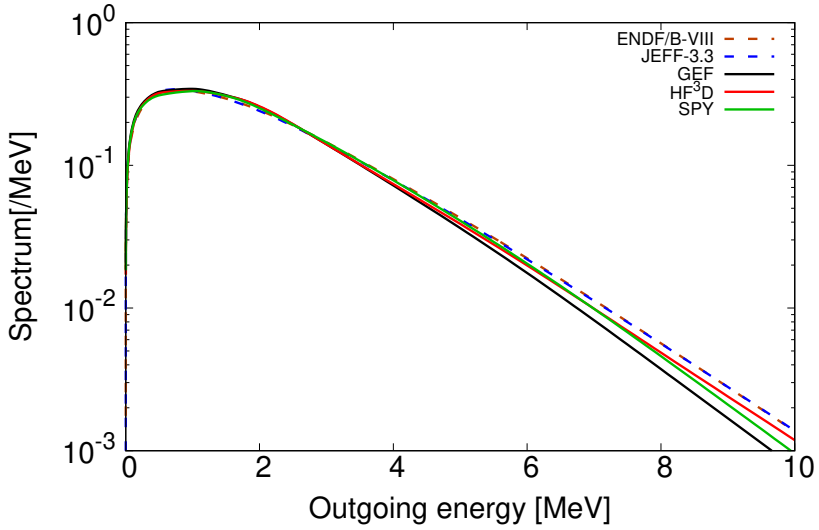

Figure 12: The incident energy dependence of an average number of neutrons.

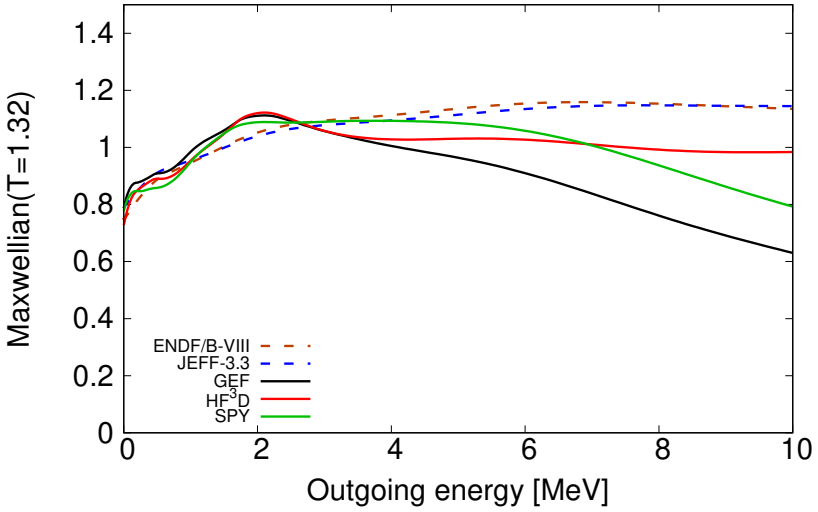

Figure 13: The incident energy dependence of an average number of neutrons.

4.2 Energy dependence

The incident energy dependence of calculated $\overline{\nu}$ are shown in Fig. 14 together with experimental and evaluated data. The calculated $\overline{\nu}$ for the SPY model are 1 larger than other data in entire incident energy range. This is due to the larger excitation energies of fission fragments produced by the SPY model than that of the other models.

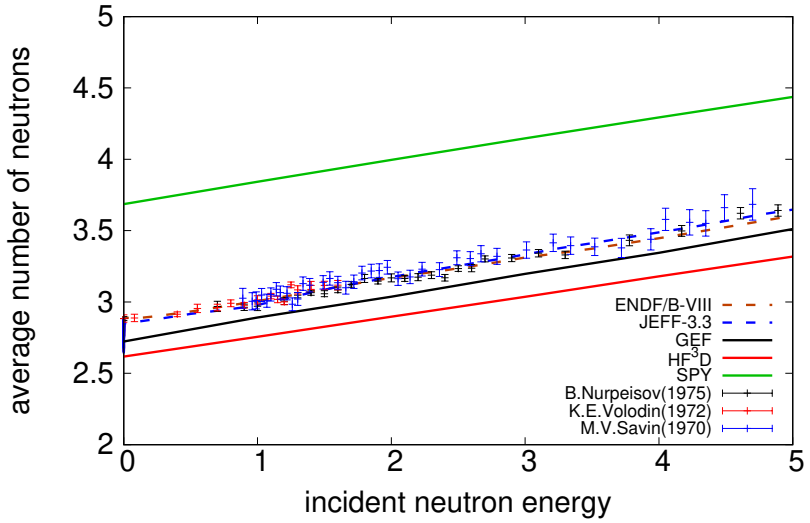

Figure 14: The incident energy dependence of an average number of neutrons.

4.3 Input keyword sensitivities

We report sensitivity analysis, that determines how different input keyword values affect a fission observables, using `Rfiseps`, `bins`, and `ldmodel` as variables. (See TALYS manual for the details of these keywords.) We use the GEF model as the example.

4.3.1 Yield cut-off: `Rfiseps`

The keyword, `Rfiseps`, is the lower limit of the fission fragment in the unit of the cross-section that is used in the calculation. It is also expected to significantly affect the calculated yields, the number of fission fragments, and thus the number of emitted prompt neutrons. Figure 15 shows the calculated fission observables by decreasing `Rfiseps` from 1.0E-02 down to 1.0E-09. The decrease in the `Rfiseps` value means the increase in the number of fission fragments being taken into account in the calculation. For the case of `Rfiseps` is 1.0E-02, many fission fragments around the symmetric region are omitted from the calculation and the $\overline{\nu}(A)$ loses continuity, while P_ν and PFNS are less sensitive for the `Rfiseps`. Generally, major evaluated fission yield libraries contain the fission product yield even less than 10^{-10}, therefore we take 1.0E-09 as a default, although the calculated results with less than 1.0E-09 does not look any different in $Y_{\rm I}(A)$ and $\overline{\nu}(A)$.

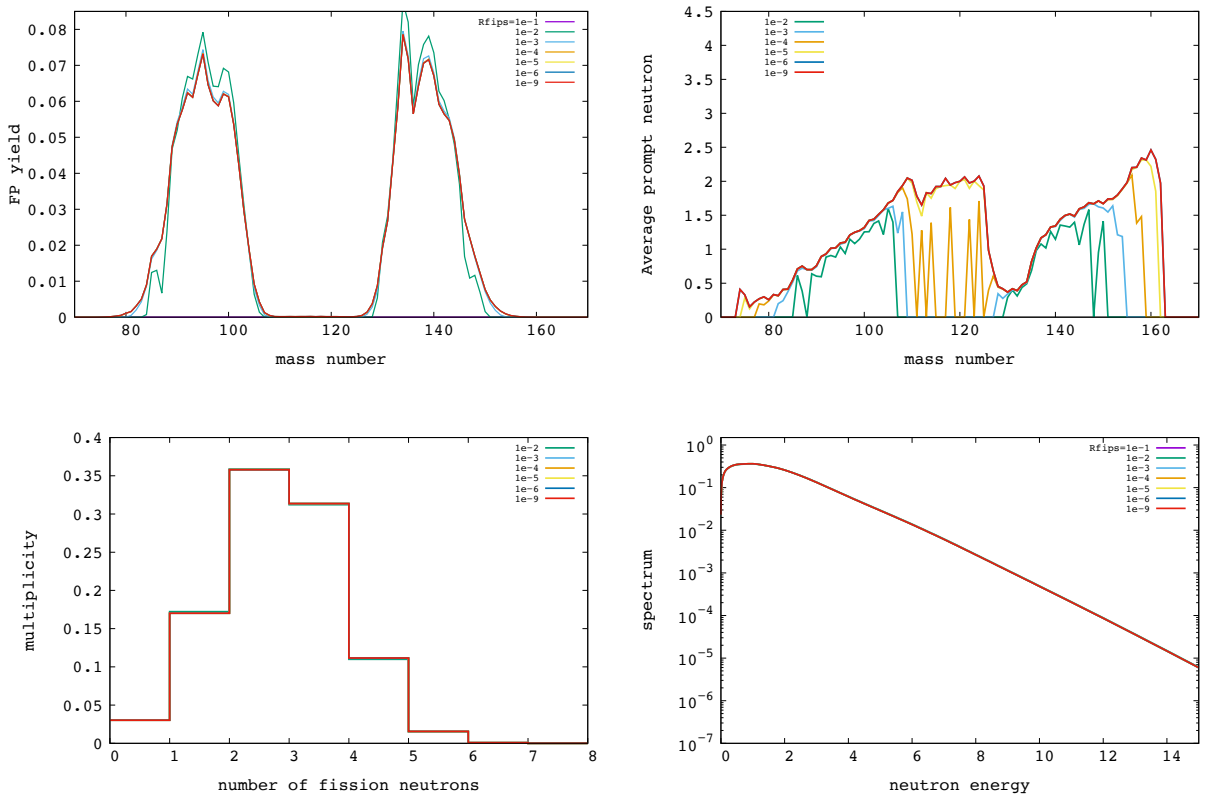

Figure 15: Input keyword sensitivities of `Rfiseps` $Y_{\rm I}(A)$ (left top), $\overline{\nu}(A)$ (right top), P_ν (left bottom), and PFNS (right bottom).

4.3.2 Excitation energy bins: `bins`

The excitation energy bins, `bins`, which is the number of divisions between the last discrete level and the total excitation energy for the initial compound nucleus. This parameter is expected to affect the energy release of fission fragments coarse or fine. As shown in Fig. 16, `bins` does not have a large effect on $Y_{\rm I}(A)$ while the neutron observables change with increasing `bins` value and are saturated above 60. Therefore, in this report, we use `bins` = 60 for all calculations.

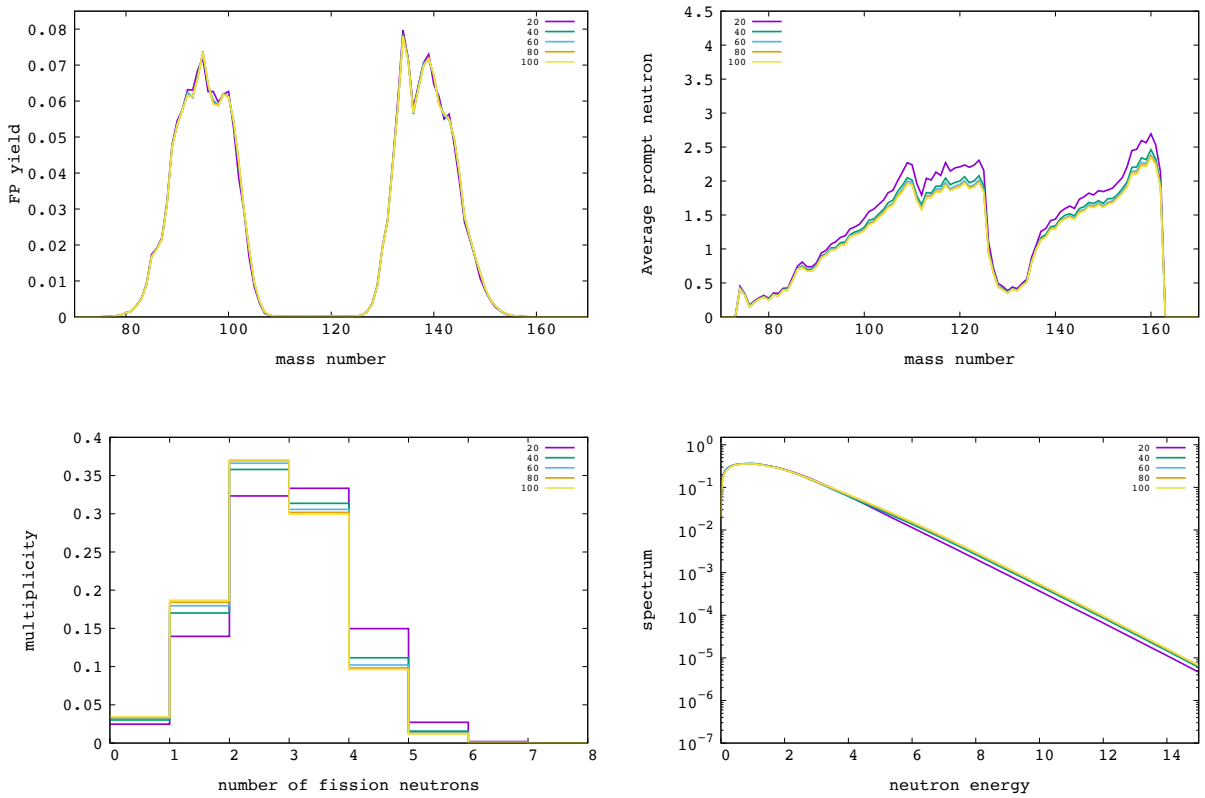

Figure 16: Input keyword sensitivities of $20 \leq$ `bins` ≤ 100 on $Y_{\mathrm{I}}(A)$ (left top), $\overline{\nu}(A)$ (right top), P_{ν} (left bottom), and PFNS (right bottom).

4.3.3 Level density model: `ldmodel`

The level density model is another important variables for the fission fragment evapolation calculation. The `ldmodel` $= 1, 2, 3$ are Constant Temperature + Fermi gas model (CTM), Back-shifted Fermi gas Model (BFM), and Generalised Superfluid Model (GSM), respectively, and `ldmodel` ≥ 4 are from theoretical models. In this report, we examine $1 \leq$ `ldmodel` ≤ 5.

Figure 17 shows the calculated results by changing `ldmodel` in the input. For the case of `ldmodel` $= 3$, it gives significant difference in $Y_{\mathrm{I}}(A)$ at the heavy mass region as well as $\overline{\nu}(A)$ and probability of neutron multiplicity distribution. For `ldmodel` $= 5$ case, the neutron emissions from light fragments surpress compared to that of the other `ldmodel`, and as a result the probability of neutron multiplicity distribution is also different trend than the other `ldmodel`. There is a large difference in the high-energy tail of PFNS between `ldmodel` $= 1$ and `ldmodel` $= 2, 3$. In this report, we use `ldmodel` $= 1$ as a default so that we can compare the calculated results to that of by the other Hauser-Feshbach based codes.

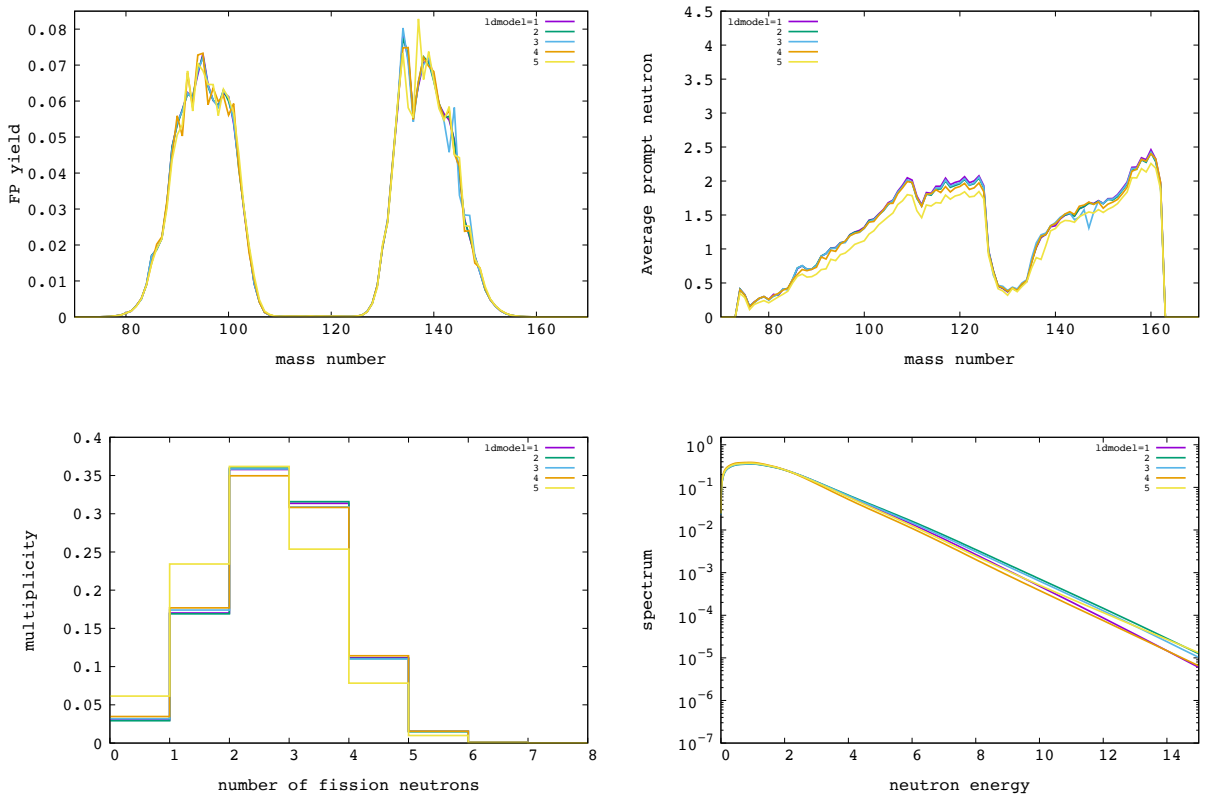

Figure 17: Input keyword sensitivities of `ldmodel` $Y_{\mathrm{I}}(A)$ (left top), $\overline{\nu}(A)$ (right top), the P_{ν} (left bottom), and PFNS (right bottom).

5 β decay

5.1 Stand alone Python β-decay module

The fission products undergo β decay after prompt neutrons and γ emissions. They also emit β- and γ-rays while β decaying. Additionally, some neutron-rich nuclides, so-called delayed neutron precursors, emit β-delayed neutron with a very small probability P_n. Figure 18 shows the β-decay scheme of A=141. The independent yields, which is produced directly after the prompt emission decay, accumulate to the cumulative yields by following the decay chain, and the build-up yields at the final nuclide in the $beta$-decay chain in the same A is called mass chain yield.

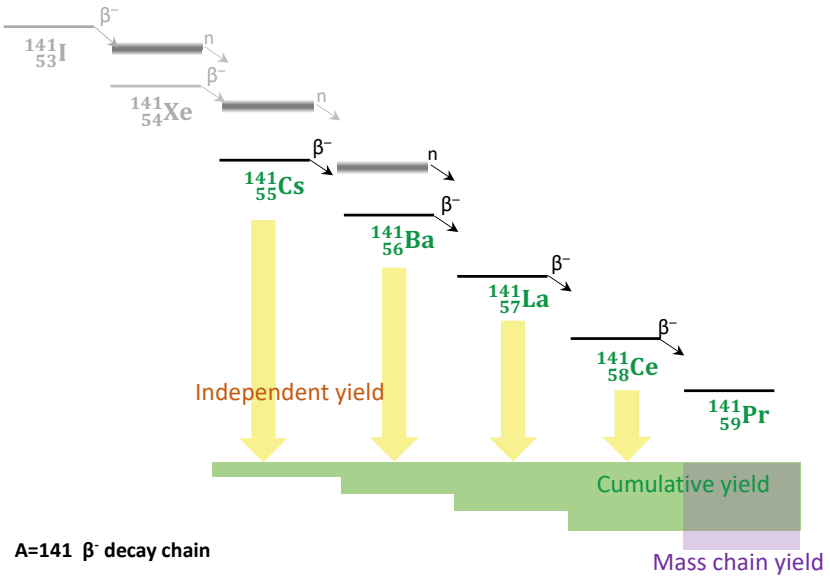

Figure 18: β-decay scheme of A=141 accompanied by delayed neutron emissions.

The time evolution of nuclide yield undergoing a linear decay chain is governed by a set of a first-order differential equations, called Bateman equations [25]. The Bateman equations for radioactive decay case of i-nuclide series in linear chain describing nuclide yield are as follows:

$$\begin{aligned} \frac{dN_1}{dt} &= -\lambda_1 N_1(t) \\ \frac{dN_i}{dt} &= \lambda_{i-1} N_{i-1}(t) - \lambda_i N_i(t) \quad (i = 2, n) \,, \end{aligned} \tag{13}$$

where λ_i is the decay constant of ith nuclide. By assuming zero yields of all progeny after time t, the yield of nth nuclide in the specific decay chain is given by:

$$\begin{aligned} N_n(t) &= \frac{N_1(0)}{\lambda_n} \sum_{i=1}^{n} \lambda_i c_i e^{(-\lambda_i t)} \\ c_n &= \sum_{j=1, i \neq j}^{n} \frac{\lambda_j}{\lambda_j - \lambda_i} \,, \end{aligned} \tag{14}$$

where C is the length of the decay chain and the decay chain must be linearized like shown in Fig. 19. Such decay chain is produced from the evaluated decay data libraries [26, 27, 28]. The

Bateman equations usually assume that a decay chain involves no branching (*i.e.* linear) and that there are only nuclides with a unique λ in the chain, so one needs to linearize all possible decay paths. If there is the same λ, infinite terms appear in the equation, thus the sum does not converge. The presence of infinities does not affect a lot in our case to estimate bulk β-decay observables, so we artificially shift the constants 0.001% that are equal and obtain an approximate solution [29].

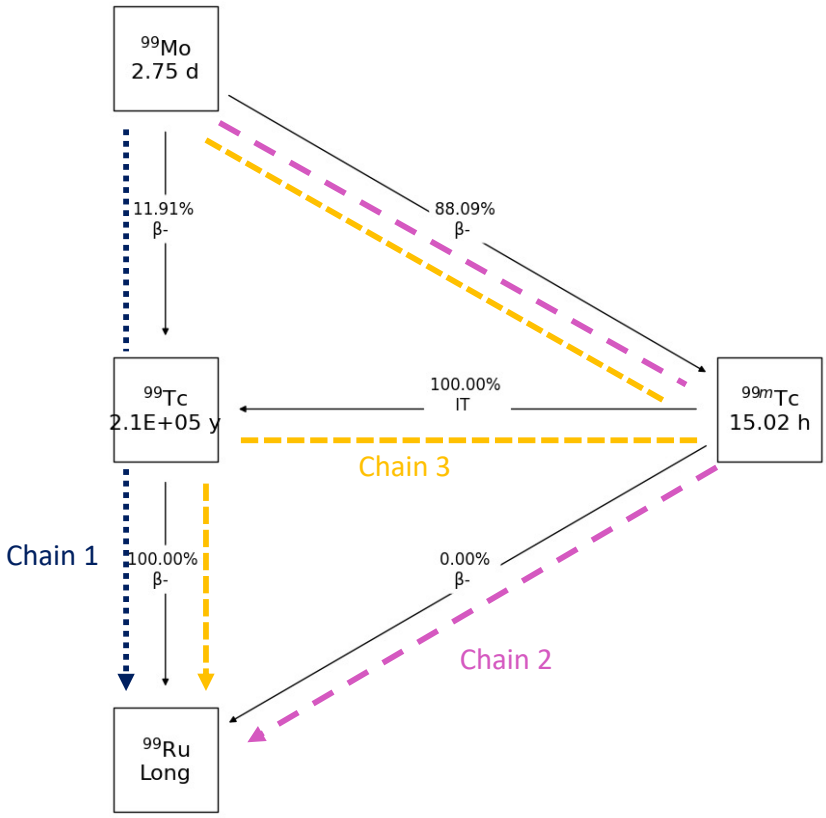

Figure 19: β-decay chain of ^{99}Mo.

In order to calculate decay heats, the average energies of β and γ components $\langle E_{\beta,\gamma} \rangle$ from fission products are imported from the evaluated decay data libraries, and the weighted sums of them as a function of time t following a single fission event are calculated based on the yield from the solution of the Bateman equation $N_i(t)$ as follows:

$$\mathrm{DH}_{\beta,\gamma}(t) = \sum_{\beta,\gamma} \langle E_{\beta,\gamma} \rangle \lambda_{\beta,\gamma} N_i(t) \tag{15}$$

Similarly, delayed neutron yields ν_d as a function of time t and the average total delayed neutron emission $\overline{\nu}_d$ at a long enough time (t=1000y) from independent fission products can be calculated by:

$$\nu_d(t) = \sum P_n \lambda_n N_i(t) \tag{16}$$

$$\overline{\nu_d} = \sum P_n N_i(t) \quad (t = 1,000y)\ . \tag{17}$$

5.2 Calculated β-decay observables from TALYS' independent fission product yields

We further asses independent fission yields calculated by TALYS with `ffmodel 1 + fymodel 4` for ^{239}Pu(n_{th},f) by calculating β-decay observables. For this purpose, the standalone Python β-decay code described above is employed. The JENDL2015 decay data library is used for the decay information and average β and γ energy releases $\langle E_{\beta,\gamma} \rangle$.

5.3 Thermal neutron induced fission

Figure 20 shows the β (top left), γ (top right) components and total decay heat, and delayed neutron yields as a function of cooling time after a fission burst. In the legends, "GEF+TALYS" and "JENDL-5", stand for calculated results using independent fission yields calculated by TALYS with `ffmodel 1` and `fymodel 4` and independent fission yields data in JENDL-5.0, respectively. For the decay heats, β (top left), γ (top right) components and total well reproduce the experimental data, while the delayed neutron yields are overestimated at all time steps compared to JENDL-5.

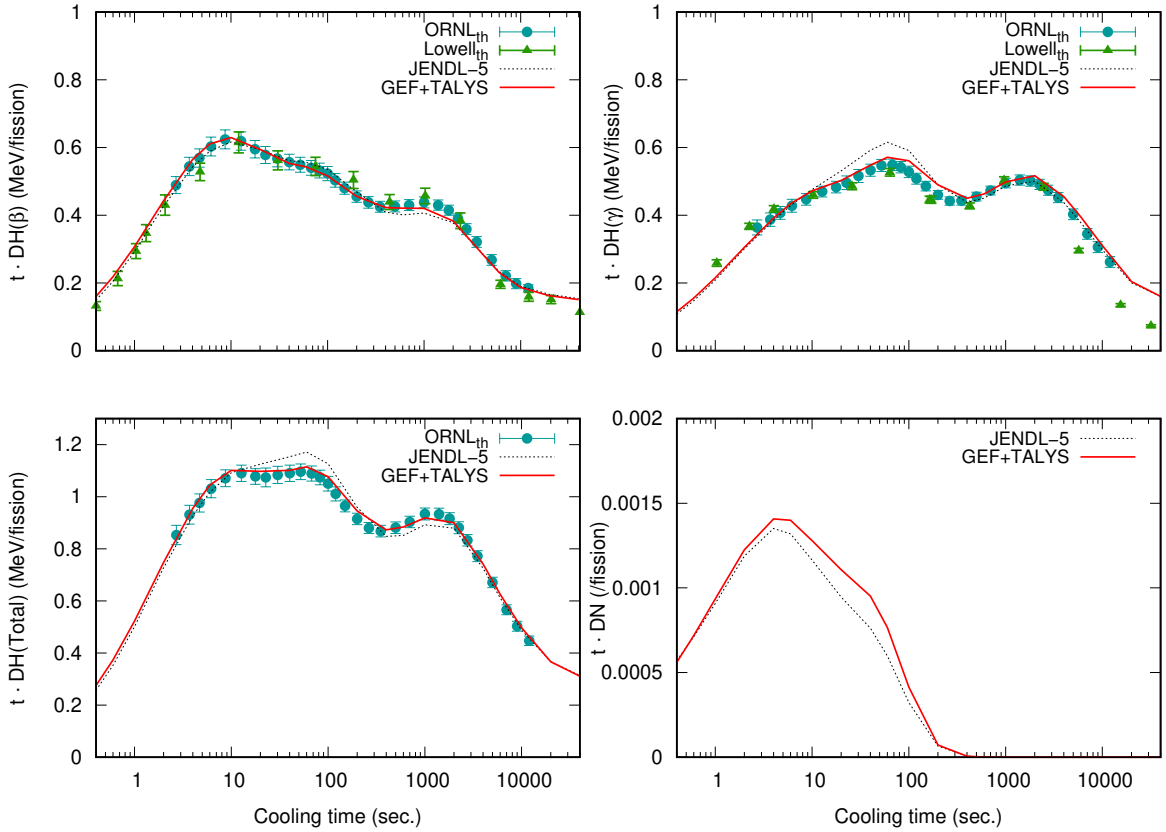

Figure 20: β (top left), γ (top right) components, and total (bottom left) of decay heats and delayed neutron yield (bottom right) as a function of cooling time calculated using ^{239}Pu(n_{th},f) independent fission product yields from TALYS output using GEF model.

5.4 Energy dependence

The calculated decay heats and delayed neutron yields for the incident neutron energies from 1 to 5 MeV are shown in Fig. 21. Though the experimental data of the incident neutron energy dependence are not readily accessible, we see the tendency of decreasing with increasing the

incident neutron energy for the decay heats. This can be explained as follows: The asymmetric distributions of fission product mass distribution is well-known for the fissioning system such as ^{235}U(n_{th},f) or ^{239}Pu(n_{th},f), and it becomes considerably broader at higher neutron energy. Then the decay heat dominant nuclides decrease as the asymmetric components decrease and symmetric components increase. For the energy dependence of delayed neutron yield, it slightly increases once at 1 MeV and then decrease with increasing the incident neutron energy.

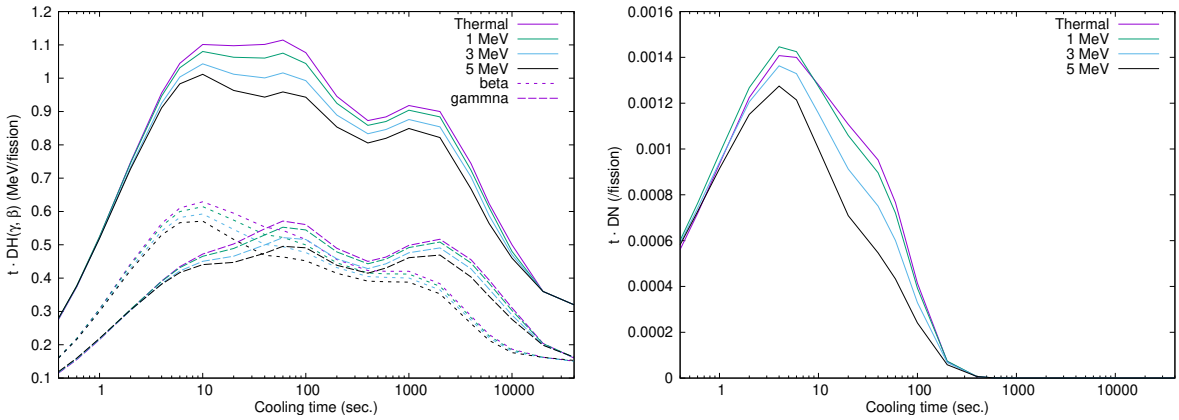

Figure 21: Calculated decay heats (left) and delayed neutron yield (right)as a function of cooling time for 1–5 MeV incident neutron energy of ^{239}Pu(n,f) independent fission product yields from TALYS output using GEF model.

The average delayed neutron yield ν_d, which is an integral of the cooling time dependent delayed neutron yield shown in Fig. 21 (left), as a function of incident neutron energy is shown in Fig. 22. Generally, the delayed neutron yields are very sensitive to the yields of so-called "delayed neutron precursors" such as $^{91-97}$Rb, however, we don't fit any data to reproduce these β-decay observables, which is out of the scope of this report.

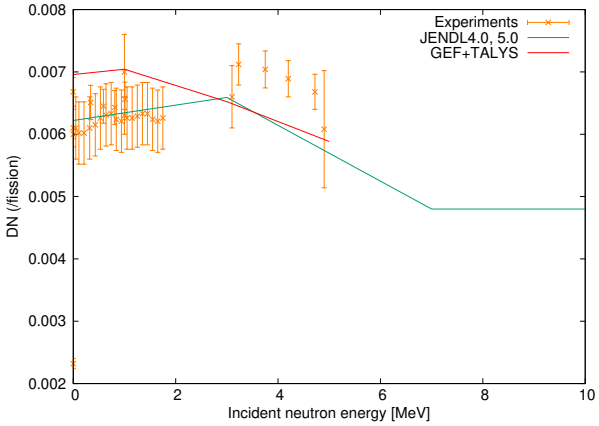

Figure 22: Delayed neutron yields as a function of incident neutron energy (MeV).

6 Summary

In this report, we described the capability of the deexcitation process for fission fragments calculating with the Hauser-Feshbach statistical decay theory in the nuclear reaction code, TALYS. The implementation is important for the nuclear data evaluation work, where consistent and correlated fission observables are required.

Three different fission fragment models, GEF, HF^{3}D, and SPY are available for currently TALYS (version 1.96) as inputs of fission fragments distribution, which is characterized by mass A, charge Z, total excitation energy (TXE), spin J, and parity Π, $Y_{\rm ff}(A, Z, \mathrm{TXE}, J, \Pi)$. For users' sake, TALYS also read the users' original distribution in files produced by theoretical or phenomenological fission fragment models to assess their competencies.

We calculated prompt neutron fission observables at incident neutron energy from thermal to 5 MeV. The results for ^{239}Pu + n reaction starting with GEF (`ffmodel 1`), HF^{3}D (`ffmodel 2`), and SPY (`ffmodel 3`) model fission fragment distribution parameters and the Hauser-Feshbach statistical decay (`fymodel 4`) calculation are shown. We see the characteristics of fission fragment distribution models from the calculated results. The agreement with experimental and evaluated data can be seen for independent fission product mass yield $Y(A)$, $\bar{\nu}$, and $P(\nu)$ for GEF and HF^{3}D models' cases. For the result starting with the SPY model, since the starting fission fragments have large yields around the symmetric region ($A = 120$) compared to GEF and HF^{3}D models, the prompt neutron observables tend to be overestimated.

Additionally, we connected the calculated independent fission product yields for ^{239}Pu + n reaction starting with GEF (`ffmodel 1`) and the Hauser-Feshbach statistical decay (`fymodel 4`) calculation to the standalone β-decay code. The results reproduced the β and γ decay heat components, while the delayed neutron yields are somehow overestimated in low incident neutron energy compared to that of experimental and evaluated data.

We will look into the details of the prompt fission neutron spectra (PFNS) and the γ observables anytime soon, and will implement the multi-chance fission energy regions as well as spontaneous and the other projectiles induced fission reactions. We also will improve and extend the fission fragment distribution parameters steadily. Currently, more and updated fission fragment distributions are expected for GEF and SPY model.

Acknowledgment

The authors thank A. Al-Adili (Uppsala University), S. Goriely (Université Libre de Bruxelles), J.-F. Lemaître (CEA), and T. Kawano (Los Alamos National Laboratory) for valuable discussions as well as data and code supplies.

The IAEA-NDS acknowledges the internship program “The Nuclear Regulation Human Resource Development Program (ANSET: Advanced Nuclear 3S Education and Training)” entrusted to Tokyo Institute of Technology, Tokyo, Japan by the Nuclear Regulation Agency of Japan, for supporting this work.

Reference

[1] N Schunck and L M Robledo. Microscopic theory of nuclear fission: a review. *Reports on Progress in Physics*, 79(11):116301, oct 2016.

[2] W. Hauser and H. Feshbach. The inelastic scattering of neutrons. *Phys. Rev.*, 87:366–373, Jul 1952.

[3] P. Talou, B. Becker, T. Kawano, M. B. Chadwick, and Y. Danon. Advanced monte carlo modeling of prompt fission neutrons for thermal and fast neutron-induced fission reactions on $^{239}\mathrm{Pu}$. *Phys. Rev. C*, 83:064612, Jun 2011.

[4] Jørgen Randrup and Ramona Vogt. Calculation of fission observables through event-by-event simulation. *Phys. Rev. C*, 80:024601, Aug 2009.

[5] O. Litaize and O. Serot. Investigation of phenomenological models for the monte carlo simulation of the prompt fission neutron and γ emission. *Phys. Rev. C*, 82:054616, Nov 2010.

[6] K.-H. Schmidt, B. Jurado, C. Amouroux, and C. Schmitt. General description of fission observables: GEF model code. *Nuclear Data Sheets*, 131:107 – 221, 2016. Special Issue on Nuclear Reaction Data.

[7] A. Tudora and F. J. Hambsch. Comprehensive overview of the Point-by-Point model of prompt emission in fission. *The European Physical Journal A*, 53(8):159, 2017.

[8] S. Okumura, T. Kawano, P. Jaffke, P. Talou, and S. Chiba. ^{235}U(n, f) independent fission product yield and isomeric ratio calculated with the statistical Hauser–Feshbach theory. *Journal of Nuclear Science and Technology*, 55(9):1009–1023, 2018.

[9] Shin Okumura, Toshihiko Kawano, Amy Elizabeth Lovell, and Tadashi Yoshida. Energy dependent calculations of fission product, prompt, and delayed neutron yields for neutron induced fission on 235u, 238u, and 239pu. *Journal of Nuclear Science and Technology*, 59(1):96–109, 2022.

[10] A. E. Lovell, T. Kawano, S. Okumura, I. Stetcu, M. R. Mumpower, and P. Talou. Extension of the hauser-feshbach fission fragment decay model to multichance fission. *Phys. Rev. C*, 103:014615, Jan 2021.

[11] David G. Madland and J. Rayford Nix. New calculation of prompt fission neutron spectra and average prompt neutron multiplicities. *Nuclear Science and Engineering*, 81(2):213–271, 1982.

[12] T. R. England and B.F. Rider. Evaluation and compilation of fission product yields. Technical Report ENDF-349, LA-UR-94-3106, Los Alamos National Laboratory, 1994.

[13] B. Pritychenko, O. Cabellos S. Oberstedt, R. Vogt, R. Capote Noy, S. Okumura, and T. Kawano. Updating fission yield data for applications. Technical Report INDC(NDS)-0817, International Atomic Energy Agency, 2021.

[14] A.J. Koning and D. Rochman. Modern nuclear data evaluation with the talys code system. *Nuclear Data Sheets*, 113(12):2841–2934, 2012. Special Issue on Nuclear Reaction Data.

[15] F. Nordström. Benchmark of the fission channels in talys. Technical Report UPTEC ES 21016, Uppsala university, 2021.

[16] J.-F. Lemaître, S. Goriely, S. Hilaire, and J.-L. Sida. Fully microscopic scission-point model to predict fission fragment observables. *Phys. Rev. C*, 99:034612, Mar 2019.

[17] R. Capote, M. Herman, P. Obložinský, P. G. Young, S. Goriely, T. Belgya, A. V. Ignatyuk, A. J. Koning, S. Hilaire, V. A. Plujko, M. Avrigeanu, O. Bersillon, M. B. Chadwick, T. Fukahori, Z. Ge, Y. Han, S. Kailas, J. Kopecky, V. M. Maslov, G. Reffo, M. Sin, E. Sh. Soukhovitskii, and P. Talou. RIPL - reference input parameter library for calculation of nuclear reactions and nuclear data evaluations. *Nuclear Data Sheets*, 110(12):3107 – 3214, 2009.

[18] U. Brosa, H.-H. Knitter, Tie-shuan Fan, Ji-min Hu, and Shang-lian Bao. Systematics of fission-channel probabilities. *Phys. Rev. C*, 59:767–775, Feb 1999.

[19] B Jurado and K H Schmidt. Status of the general description of fission observables by the GEF code. *European Research Infrastructures for Nuclear Data Applications (ERINDA) workshop, CERN, Geneva, Switzerland, 1 - 3 Oct 2013*, 2014.

[20] A. C. Wahl. Systematics of fission-product yields. Technical Report LA-13928, Los Alamos National Laboratory, 2002.

[21] T. Ohsawa, T. Horiguchi, and M. Mitsuhashi. Multimodal analysis of prompt neutron spectra for ^{238}Pu(sf), ^{240}Pu(sf), ^{242}Pu(sf) and ^{239}Pu(n_{th},f). *Nuclear Physics A*, 665(1):3 – 12, 2000.

[22] A. C. Wahl. Nuclear-charge distribution and delayed-neutron yields for thermal-neutron-induced fission of ^{235}U, ^{233}U, and ^{239}Pu and for spontaneous fission of ^{252}Cf. *Atomic Data and Nuclear Data Tables*, 39(1):1 – 156, 1988.

[23] S. Goriely, N. Chamel, and J. M. Pearson. Hartree-fock-bogoliubov nuclear mass model with 0.50 mev accuracy based on standard forms of skyrme and pairing functionals. *Phys. Rev. C*, 88:061302, Dec 2013.

[24] J.-F. Lemaître. Private communication.

[25] H. Bateman. Solution of a system of differential equations occurring in the theory of radioactive transformations. *Proc. Cambridge Philos. Soc.*, 15:423—-427, 1910.

[26] K. Shibata, O. Iwamoto, T. Nakagawa, N. Iwamoto, A. Ichihara, S. Kunieda, S. Chiba, K. Furutaka, N. Otuka, T. Ohsawa, T. Murata, H. Matsunobu, A. Zukeran, S. Kamada, and J. Katakura. JENDL-4.0: A New Library for Nuclear Science and Engineering. *J. Nucl. Sci. Technol.*, 48:1 – 30, Jan 2011.

[27] Jeff-3.3. Technical report, OECD/Nuclear Energy Agency, 2017.

[28] D. A. Brown, M. B. Chadwick, R. Capote, A. C. Kahler, A. Trkov, M. W. Herman, A. A. Sonzogni, Y. Danon, A. D. Carlson, M. Dunn, D. L. Smith, G. M. Hale, G. Arbanas, R. Arcilla, C. R. Bates, B. Beck, B. Becker, F. Brown, R. J. Casperson, J. Conlin, D. E. Cullen, M. A. Descalle, R. Firestone, T. Gaines, K. H. Guber, A. I. Hawari, J. Holmes, T. D. Johnson, T. Kawano, B. C. Kiedrowski, A. J. Koning, S. Kopecky, L. Leal, J. P. Lestone, C. Lubitz, J. I. Márquez Damián, C. M. Mattoon, E. A. McCutchan, S. Mughabghab, P. Navratil, D. Neudecker, G. P. A. Nobre, G. Noguere, M. Paris, M. T. Pigni, A. J. Plompen, B. Pritychenko, V. G. Pronyaev, D. Roubtsov, D. Rochman, P. Romano, P. Schillebeeckx, S. Simakov, M. Sin, I. Sirakov, B. Sleaford, V. Sobes, E. S. Soukhovitskii, I. Stetcu, P. Talou, I. Thompson, S. van der Marck, L. Welser-Sherrill, D. Wiarda, M. White, J. L.

Wormald, R. Q. Wright, M. Zerkle, G. Žerovnik, and Y. Zhu. ENDF/B-VIII.0: The 8th Major Release of the Nuclear Reaction Data Library with CIELO-project Cross Sections, New Standards and Thermal Scattering Data. *Nuclear Data Sheets*, 148:1 – 142, 2018.

[29] K. Oyamatsu, H. Takeuchi, M. Sagisaka, and J. Katakura. New method for calculating aggregate fission product decay heat with full use of macroscopic-measurement data. *Journal of Nuclear Science and Technology*, 38(7):477–487, 2001.